Journal of Physiology (2002), **538.2**, *pp.* 541–553
DOI: 10.1013/jphysiol.2001.012856

www.jphysiol.org

Non-invasive magnetic resonance imaging assessment of myocardial changes and the effects of angiotensin-converting enzyme inhibition in diabetic rats

Ahmad I. M. Al-Shafei *†, R. G. Wise *‡, G. A. Gresham *, G. Bronns §, T. A. Carpenter ¶, L. D. Hall * and Christopher L.-H. Huang †

** Herchel Smith Laboratory for Medicinal Chemistry, University of Cambridge School of Clinical Medicine, Forvie Site, Robinson Way, Cambridge CB2 2PZ, † Physiological Laboratory, Department of Physiology, University of Cambridge, Downing Site, Downing Street, Cambridge CB2 3EG, ‡ Oxford Centre for Functional Magnetic Resonance Imaging of the Brain, University of Oxford, John Radcliffe Hospital, Headington, Oxford OX3 9DU, § Department of Surgery, Box 202, Level 9, Addenbrooke's Hospital, Cambridge CB2 2QQ and ¶ The Wolfson Brain Imaging Centre, University of Cambridge, Box 65, Addenbrooke's Hospital, Cambridge CB2 2QQ, UK*

A non-invasive cine magnetic resonance imaging (MRI) technique was developed to allow, for the first time, detection and characterization of chronic changes in myocardial tissue volume and the effects upon these of treatment by the angiotensin-converting enzyme (ACE) inhibitor captopril in streptozotocin (STZ)-diabetic male Wistar rats. Animals that had been made diabetic at the ages of 7, 10 and 13 weeks and a captopril-treated group of animals made diabetic at the age of 7 weeks were scanned. The findings were compared with the results from age-matched controls. All animal groups ($n = 4$ animals in each) were consistently scanned at 16 weeks. Left and right ventricular myocardial volumes were reconstructed from complete data sets of left and right ventricular transverse sections which covered systole and most of diastole using twelve equally incremented time points through the cardiac cycle. The calculated volumes remained consistent through all twelve time points of the cardiac cycle in all five experimental groups and agreed with the corresponding post-mortem determinations. These gave consistent myocardial densities whose values could additionally be corroborated by previous reports, confirming the validity of the quantitative MRI results and analysis. The myocardial volumes were conserved in animals whose diabetes was induced at 13 weeks but were significantly increased relative to body weight in animals made diabetic at 7 and 10 weeks. Captopril treatment, which was started immediately after induction of diabetes, prevented the development of this relative hypertrophy in both the left and right ventricles. We have thus introduced and validated quantitative MRI methods in a demonstration, for the first time, of chronic myocardial changes in both the right and left ventricles of STZ-diabetic rats and their prevention by the ACE inhibitor captopril.

(Received 13 June 2001; accepted after revision 28 September 2001)
Corresponding author C. L.-H. Huang: Department of Physiology, University of Cambridge, Downing Site, Downing Street, Cambridge CB2 3EG, UK. Email: clh11@cus.cam.ac.uk

There have been suggestions that both insulin-dependent and non-insulin-dependent diabetes mellitus are associated with a specific diabetic cardiomyopathy (Ledet, 1968, 1976; Goodwin & Oakley, 1972; Rubler *et al.* 1972; Garcia *et al.* 1974; Hamby *et al.* 1974; Paz-Guevara *et al.* 1975; Crall & Roberts, 1978; Kannel & McGee, 1979; Ledet *et al.* 1979; Kannel, 1985; Bell, 1995). This might account for the increased incidence of congestive cardiac failure which exceeds that attributable to the coronary artery disease, hypertension and cardiac autonomic neuropathy prevalent in diabetes (Kannel *et al.* 1974). Histological studies have reported myocyte hypertrophy that might reflect primary changes associated with the condition (Rubler *et al.* 1972; Fischer *et al.* 1979). Human diabetic hearts can also become fibrotic due to collagen accumulation (Rubler *et al.* 1972; Regan, 1981). These primarily myocardial changes occurred independently of, or accompanied, coronary microcirculatory abnormalities. The latter included basal laminar thickening, endothelial cell proliferation, sub-endothelial fibrosis, periodic acid–Schiff-positive (PAS-positive) deposition with vessel luminal narrowing and wall thickening (Blumenthal *et al.* 1960; Ledet, 1968, 1976; Vracko & Benditt, 1970; Rubler *et al.* 1972; Hamby *et al.* 1974; Williamson & Kilo, 1976; Seneviratne, 1977; Sanderson *et al.* 1978; Fischer *et al.* 1979; Zoneraich *et al.* 1980).

However, clinical echocardiographic studies seeking physiological correlates for such changes variously reported reduced (Airaksinen *et al.* 1984, 1987), normal or modestly increased (Shapiro *et al.* 1981; Friedman *et al.* 1982) left ventricular size. Exploration of experimental

diabetic models would permit closer control of disease timing, severity and experimental conditions but has hitherto relied on conventional invasive physiological or *in vitro* techniques with their associated restrictions upon serial studies in chronic systems (e.g. Regan *et al.* 1974; Hearse *et al.* 1975; Miller, 1979; Feuvray *et al.* 1979; Fein *et al.* 1980; Warley *et al.* 1995; Riva *et al.* 1998). In the present studies (see also the accompanying paper Al-Shafei *et al.* 2002) non-invasive MRI techniques have accordingly been developed to detect and characterize chronic myocardial changes in the ventricular walls in the chronic streptozotocin (STZ)-diabetic rodent model. Rats were made diabetic at similar ages (7, 10 and 13 weeks) to those used in earlier anatomical and physiological studies which employed the same experimental model. Similarly, imaging took place at an age (16 weeks) largely in accord with the ages adopted in the previous investigations (13–17 weeks, see references below). The present MRI findings are therefore comparable with earlier anatomical and physiological characterizations using conventional invasive techniques. For example, earlier anatomical studies examined for light microscopic evidence of interstitial fibrosis (Factor *et al.* 1981) and ultrastructural changes (Jackson *et al.* 1985; Warley *et al.* 1995) over similar age periods. There have also been physiological studies of papillary muscle function (Fein *et al.* 1980; Fein & Sonnenblick, 1994; Warley *et al.* 1995), myocardial contraction and relaxation (Jackson *et al.* 1985; Afzal *et al.* 1988), diastolic and peak systolic pressures (Miller, 1979; Rodrigues & McNeill, 1986; Paulson *et al.* 1987; Afzal *et al.* 1988; Rodrigues *et al.* 1988; Lopaschuk & Spafford, 1989; Shimabukuro *et al.* 1995; Goyal *et al.* 1998) and heart rates (Jackson & Carrier, 1983; Afzal *et al.* 1988; Hicks *et al.* 1998).

System hardware and MRI pulse sequences were modified for the reliable imaging of rapidly beating rodent hearts whilst minimizing motion artefacts. The use of gradient-echo cine magnetic resonance imaging clearly demarcated myocardium from blood in the cardiac chambers (Rehr *et al.* 1985; Higgins, 1986; Stratemeier *et al.* 1986; Caputo *et al.* 1987; Markiewicz *et al.* 1987; Pettigrew, 1989; Sechtem *et al.* 1987; Utz *et al.* 1987, 1988; Pflugfelder *et al.* 1989; Semelka *et al.* 1990). This gave images that permitted a quantitative reconstruction of the cardiac anatomy from serial transverse cardiac sections obtained in a procedure that offered reproducibly defined imaging planes. The resulting assessments of myocardial hypertrophy proved internally consistent within each individual imaging session and the results agreed with conventional morphological determinations. They thus successfully used MRI methods to demonstrate for the first time that chronic diabetic cardiomyopathy alters overall myocardial volume.

This experimental system was then applied to assess how the angiotensin-converting enzyme (ACE) inhibitor captopril influenced such chronic myocardial alterations. This investigation was prompted by suggestions of an intracardiac renin–angiotensin system (Dostal *et al.* 1992*a*,*b*) and its activation in diabetes (Rösen *et al.* 1995). STZ-diabetic rats show increased left ventricular ACE levels and decreased left ventricular developed pressures; the latter were prevented by enalapril (Goyal *et al.* 1998). Angiotensin II in turn induces growth responses in isolated adult rat hearts (Schunkert *et al.* 1995), hypertrophy in isolated neonatal rat ventricular myocytes (LaMorte *et al.* 1994) and cardiac fibroblast proliferation *in vitro* (Schorb *et al.* 1993, 1994; Crabos *et al.* 1994; Matsubara *et al.* 1994). These actions could cause the myocardial interstitial fibrosis reported in some forms of cardiac hypertrophy and cardiomyopathies that in turn diminish myocardial compliance. Angiotensin II system abnormalities may also impair myocardial contractility and disturb coronary blood flow regulation in diabetics (Weber & Brilla, 1991; Dostal *et al.* 1992*a*,*b*).

Such experiments provided the first non-invasive physiological evidence that the ACE inhibitor captopril ameliorates the myocardial hypertrophic changes. Clinical evidence suggests that ACE inhibitors exert beneficial effects in hypertensive cardiac disease and on left ventricular performance in congestive heart failure (Cohn & Levine, 1982; Kluger *et al.* 1982; Levine *et al.* 1982), rectify the abnormal resistance vessel structure in essential hypertension (Mulvany, 1992, 1998), increase arterial wall compliance (Dzau & Safar, 1988) and reverse vascular and left ventricular hypertrophy (Dunn *et al.* 1984). The present findings justify testing for similar therapeutic physiological effects in diabetic cardiac disease, in addition to providing the MRI techniques for the more acute physiological analyses of cardiac cycle changes in the diabetic cardiac disease model detailed in the accompanying paper (Al-Shafei *et al.* 2002).

METHODS

Design of experimental protocols

All animal procedures used protocols approved by the Home Office, UK, in accordance with the Animal Scientific Procedures Act (1986). A total of 20 male fully conditioned, healthy, pathogen-free Wistar rats (6 weeks old; Harlan, UK) were reared by the University of Cambridge Central Biomedical Service under standard housing conditions and fed a normal animal chow with water *ad libitum*. The animals were divided randomly into five experimental groups (each $n = 4$ rats). Diabetes was induced in four of the groups as described below (2 groups at 7 weeks old, 1 at 10 weeks old and 1 at 13 weeks old). The fifth group was kept as a control.

All animals in both test and control groups were scanned at 16 weeks. Induction of diabetes at 7, 10, and 13 weeks concurred with induction of diabetes employed in previous studies (see Introduction) and allowed investigation the effect of age of induction of diabetes on the development of structural and functional changes in both ventricles. For one of the two groups in

which diabetes was induced at 7 weeks, captopril (Sigma-Aldrich Co., Poole, Dorset, UK) was added to the drinking water at a concentration of 2 g l^{-1} immediately after STZ treatment (Dalton *et al.* 1997; Qi *et al.* 1999); this continued until they were scanned at 16 weeks. This made it possible to evaluate the effects of captopril on the cardiac changes produced by diabetic cardiomyopathy. The rats in the control group were imaged at 16 weeks and provided age- and sex-matched controls for all four diabetic groups.

The rats in each of the four experimental groups were first anaesthetized using 1–2 % halothane (Sigma-Aldrich Co. Poole, Dorset, UK) in oxygen (British Oxygen Gas, UK) and their blood glucose levels measured using a blood glucometer. This was followed by a single intraperitoneal streptozotocin injection (Junod *et al.* 1967, 1969). Streptozotocin (STZ: 65 mg (kg body weight)$^{-1}$; Sigma-Aldrich Co. Poole, Dorset, UK) was dissolved in phosphate-buffered saline to which a few drops of citric acid (10 g (100 ml)$^{-1}$) were added to give a pH of 4.5. This precaution was adopted to prevent the rapid inactivation of STZ at a neutral pH (see Junod *et al.* 1967). The control rats received sham injections of the citrated buffer under halothane anaesthesia when they were 7 weeks old. STZ at a dose of 55–65 mg (kg body weight)$^{-1}$ is known to produce severe but stable diabetes in Wistar rats (Lopaschuk *et al.* 1983; Warley *et al.* 1995; Rodrigues *et al.* 1990, 1997). Hyperglycaemia (blood glucose level > 13 mM) ensued 48 h post STZ. The body weight of all animals was monitored every 3 days and blood glucose level every 2 weeks using a glucometer. Blood glucose levels of STZ-injected rats measured 2 weeks after injection always exceeded 13 mM.

Physiological monitoring methods

Rats were anaesthetized using 1–2 % halothane (Sigma-Aldrich Co. Poole, Dorset, UK) in oxygen (British Oxygen Gas, UK), prior to each imaging session. Their systolic blood pressures were measured using a non-invasive rat-tail blood pressure monitor (Harvard Apparatus, Edenbridge, Kent, UK) and are summarized in Tables 1 and 4. This measurement was repeated immediately after the MRI session to confirm its stability within reasonable physiological limits. Shielded subcutaneous electrodes were used for electrocardiographic (ECG) recording and display using a Tektronix 2225 oscilloscope (Tektronix, Harpenden, Herts, UK). These signals permitted imaging acquisition to be synchronized or gated to the electrocardiographic QRS thus minimizing movement artefacts, and heart rate to be monitored throughout the imaging sessions. Following establishment of stable ECG trigger signals, the anaesthetized animal was then placed in a specially designed home-built half-sine-spaced birdcage radio-frequency (RF) probe (Ballon *et al.* 1990).

Magnetic resonance imaging hardware and pulse sequence

All experiments were performed in a 2 T Oxford Instruments (UK) superconducting magnet with a horizontal internal bore of 31 cm. A home-built gradient set with maximized magnetic field gradient and low resistance was used for imaging. This gradient set was of 11 cm internal diameter and fitted in the 31 cm bore of the 2 T horizontal magnet. The RF coil was a home-built half-sine-spaced birdcage probe, approximately half-cylindrical in shape, with both ends open and of internal diameter of 4.5 cm (Ballon *et al.* 1990). It fitted inside the bore of the gradient set, incorporated delivery tube assemblies that delivered anaesthetic gases and provided secure attachments for the ECG leads thus providing a self-contained assembly for the physiological monitoring of the animal lying in the RF probe which was inserted into the magnet bore for MRI.

The imaging sessions characterized both left and right ventricular anatomy throughout systole and diastole. The gated cine protocol synchronized line acquisition to set times following alternate electrocardiographic R waves. This acquisition was then repeated for the same slice position at twelve equally incremented times throughout the cardiac cycle. This sequence in turn was repeated for each of the 128 lines per slice to generate each 128 pixel × 128 pixel image, which itself was acquired twice for signal averaging. This procedure was repeated 12 times to obtain

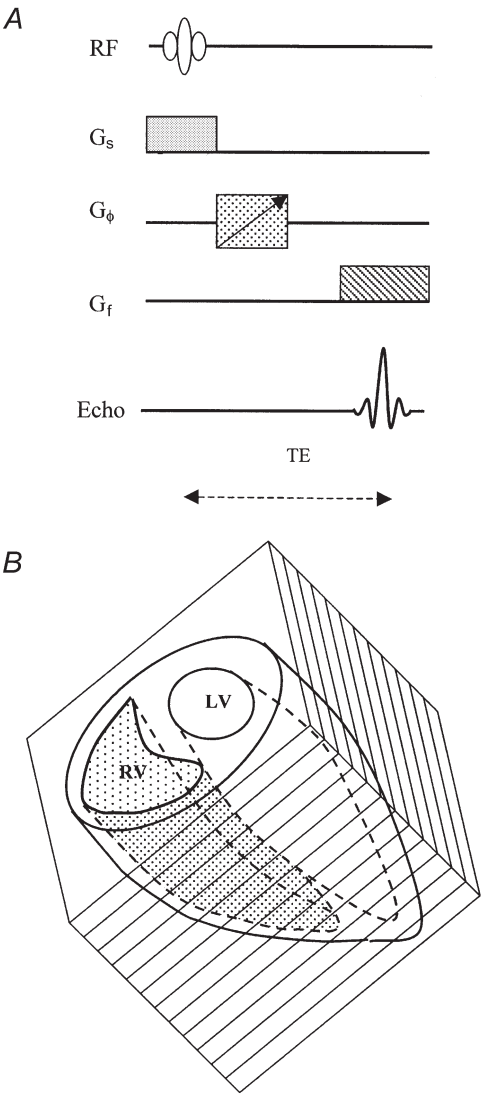

Figure 1. Gradient echo pulse sequence (*A*), and diagrammatic representation of the right and left ventricles of the rat heart (*B*)

Typically 12 transverse serial image slices, taken perpendicular to the principal cardiac axis, were acquired contiguously to image both ventricles in their entirety. Each transverse cardiac slice was typically imaged at 12 points in time during the cardiac cycle using a gated cine protocol. The pulse sequence was thus applied 12 times during each particular cardiac cycle. A full data set with MR images at the 12 time points was obtained from each particular slice before imaging other slices. Thus, the effective repeat time (TR) was 13 ms. Echo time, TE = 4.3 ms. LV and RV indicate left and right ventricles, respectively, and G_s, G_ϕ and G_f represent slice-selecting, phase-encoding and frequency-encoding gradients respectively.

Table 1. Basic physiological parameters of control rats and rats from the three diabetic groups not treated with captopril

	Control	Diabetic			*P*
		3 week	6 week	9 week	
Age at disease induction (weeks)	NA	13	10	7	NA
Body weight at disease induction (g)	NA	348 ± 8.5 †	315 ± 6.5 †	279 ± 4.3 †	NA
Body weight at scanning time (g)	351.3 ± 9.7 [c,d]	335 ± 8.4 [c,d]	282.5 ± 6.6 [a,b,d]	235 ± 8.4 [a,b,c]	< 0.001
Blood glucose (mM)	5.2 ± 0.2 [b,c,d]	29.8 ± 1.5 [a]	30.3 ± 1.8 [a]	30.9 ± 1.4 [a]	< 0.001
Systolic blood pressure (mmHg)	143.8 ± 6.3 [d]	137.5 ± 7.2 [d]	112.5 ± 7.2	93.8 ± 12 [a,b]	0.004
Heart rate (beats min^{-1})	322 ± 9 [c,d]	318 ± 7 [c,d]	280 ± 7 [a,b]	280 ± 6 [a,b]	0.002

NA, not applicable. All values are expressed as means ± S.E.M.; $n = 4$. One-way ANOVA was used to compare the control and the three untreated diabetic groups followed by Tukey's honestly significant difference test for pair-wise multiple comparisons. A value of $P < 0.05$ was considered significant. [a] Significantly different from the control group. [b] Significantly different from the 3 week diabetic group. [c] Significantly different from the 6 week diabetic group. [d] Significantly different from the 9 week untreated diabetic group. † Within accepted range of standard Wistar rat growth curves.

signal-averaged images for every slice. Each imaging session therefore required (128 × 12 × 2 × 2) times the cardiac cycle duration. The procedure thus typically obtained 12 slice images each perpendicular to the principal cardiac axis extending through the entire length of the two ventricles from the cardiac base to its apex (Fig. 1*B*). Each of the 12 slices was imaged at 12 time points covering systole and most of diastole. Imaging was successful despite the high intrinsic heart rates, which reached about 350 beats min^{-1}. The experiments used a repeat time (TR) of ~13 ms. The experiments used a short echo time (TE) of 4.3 ms to reduce motion artefacts in the images and to maximize contrast between blood and myocardium with the blood giving higher signal intensity during systole. Finally, the image data were transferred from the MRI console using in-house hardware and software to remote UNIX workstations for quantitative analysis using in-house software based on CaMReS libraries (CaMReS, Dr N. J. Herrod, Herchel Smith Laboratory for Medicinal Chemistry, University of Cambridge).

Post-mortem examination

The animals were killed after the MRI using an overdose of Euthetal (Schedule I method, Animal Scientific Procedures Act 1986) and their hearts removed and fixed in 3.7 % phosphate-buffered formaldehyde (BDH, Poole, UK) (Factor *et al.* 1981). The hearts were then removed from the fixative and blotted dry. The two atria were removed and transverse sections (1–2 mm thick) of both ventricles were cut. Right and left ventricular myocardia were then separated from each other and weighed.

RESULTS

Having established the MRI methods and the use of age-matched control and test STZ-diabetic groups of animals as described above, the experiments firstly characterized myocardial changes in both left and right ventricles associated with experimental diabetes using non-invasive MRI in an experimental design that permitted comparison of *in vivo* MRI findings to earlier *in vitro* results (see Introduction). Secondly, the experiments compared the effect of age of induction of diabetes at 7, 10 and 13 weeks. This gave rise to experimental groups that are described for convenience in the tables and figures as animals with diabetic histories of 9, 6 and 3 weeks, respectively. Thirdly, the experimental findings were used as a basis for evaluation of the possible effects of captopril in the groups that had been made diabetic at 7 weeks. Accordingly, the statistical analyses first applied a one-way analysis of variance (ANOVA) to compare the control and the three diabetic groups not treated with captopril (Tables 1–3). A second one-way ANOVA involved the control group and the two groups with diabetes induced at age 7 weeks, either treated with captopril or otherwise (Table 4). Where statistically significant differences were detected, pair-wise multiple statistical comparisons used Tukey's honestly significant difference (HSD) test with differences considered significant at $P < 0.05$. These made it possible to compare individual experimental groups with the age-matched control, as well as to assess the effect of disease onset on statistical parameters examined at a fixed age. The possible statistical significance of differences in measurements of structural parameters such as myocardial density between left and right ventricles in each of the five experimental groups was determined by Student's two-tailed paired *t* tests with differences considered significant at $P < 0.05$. Pearson's correlation coefficient (r) was used to test for correlations between measured or calculated quantities. All tables present data as means ± standard errors of the mean (S.E.M.).

Basic physiological parameters in control and diabetic animals and the effects of captopril

Basic physiological parameters measured here in the experimental STZ-diabetic model during MRI studies were in agreement with earlier findings which would indicate that our novel MRI findings are also comparable with measurements available from conventional physiological and anatomical studies (see Introduction for references). Table 1 compares these baseline parameters from the control and the different diabetic groups not treated with captopril. Table 4 summarizes the results of further analysis of data

Table 2. Left and right ventricular weights of control rats and rats from the three diabetic groups not treated with captopril

	Control	Diabetic 3 week	Diabetic 6 week	Diabetic 9 week	*P*
Left ventricular wt (g)	0.663 ± 0.01 [d]	0.645 ± 0.01 [d]	0.615 ± 0.02	0.555 ± 0.03 [a,b]	0.012
Right ventricular wt (g)	0.21 ± 0.004 [d]	0.208 ± 0.005 [d]	0.188 ± 0.006	0.176 ± 0.006 [a,b]	0.002
Left ventricular wt/body wt (%)	0.189 ± 0.002 [c,d]	0.193 ± 0.001 [c,d]	0.218 ± 0.003 [a,b,d]	0.236 ± 0.003 [a,b,c]	< 0.001
Right ventricular wt/body wt (%)	0.06 ± 0.001 [c,d]	0.062 ± 0.001 [c,d]	0.066 ± 0.001 [a,b,d]	0.075 ± 0.0004 [a,b,c]	< 0.001

Details as for Table 1. Data are means ± S.E.M.; $n = 4$.

Table 3. MRI-measured left and right ventricular myocardial volumes of control rats and rats from the three diabetic groups not treated with captopril

	Control	Diabetic 3 week	Diabetic 6 week	Diabetic 9 week	*P*
Left ventricular myocardial volume (LVMV) (μl)	653.5 ± 10.3 [d]	637.5 ± 3.9 [d]	602.5 ± 23.9	538.8 ± 20.8 [a,b]	0.003
Right ventricular myocardial volume (RVMV) (μl)	205 ± 5.4 [d]	198.8 ± 4.3 [d]	181.3 ± 5.5	169 ± 8.2 [a,b]	0.005
LVMV/body weight (μl g^{-1})	1.86 ± 0.03 [c,d]	1.9 ± 0.01 [c,d]	2.13 ± 0.04 [a,b,d]	2.29 ± 0.01 [a,b,c]	< 0.001
RVMV/body weight (μl g^{-1})	0.58 ± 0.01 [c,d]	0.59 ± 0.01 [d]	0.64 ± 0.01 [a,d]	0.72 ± 0.01 [a,b,c]	< 0.001

The left and right ventricular myocardial volume measured by MRI, for each rat, was taken from the average value from all time points sampled throughout the cardiac cycle. The body weight-normalized left and right ventricular myocardial volumes of the experimental rats were calculated using the corresponding body weight of the anaesthetised rat. Statistical details as for Table 1. Data are means ± S.E.M.; $n = 4$.

obtained from the captopril-treated diabetic animals. Firstly, Tables 1 and 4 confirm that the STZ treatment successfully resulted in significantly elevated blood glucose concentrations five- to sixfold greater than that of the control group in both the presence and absence of parallel captopril treatment. Such levels remained consistently elevated throughout the experimental period confirming severe but stable diabetes. Secondly, Table 1 shows that heart rates and systolic blood pressures were significantly reduced particularly in animals made diabetic at the earlier ages in agreement with previous studies (Maeda *et al.* 1995; Hicks *et al.* 1998). These reductions became significant compared with the control group in animals diabetic from 7 and 10 (but not 13) weeks. In contrast, Table 4 demonstrates that captopril treatment restored these cardiovascular parameters to values statistically indistinguishable from those of the control group and accordingly distinct from the heart rates and systolic blood pressures shown by similarly diabetic rats not treated with captopril. Thirdly, Tables 1 and 4 include weights of animals both at the time of disease induction, and at the time of scanning (Malhotra *et al.* 1981). Diabetes led to a fall in body weight that was greater the earlier the age of disease induction. This was again in agreement with previous reports (Pierce & Dhalla, 1981, 1983, 1985*a,b*; Afzal *et al.* 1988; see also Introduction). Student's two-tailed paired *t* test indicated significant falls in body weight at scanning compared with body weight at induction in animals made diabetic from 7 ($P = 0.003$) and 10 weeks ($P = 0.04$). Control animals showed the expected increase in weight associated with normal growth. There was no significant change in rats made diabetic at 13 weeks ($P = 0.3$) or those treated with captopril ($P = 0.53$).

Absolute and normalized left and right ventricular weights

Table 2 summarizes both the absolute left and right ventricular weights and the corresponding values normalized to body weight for all the experimental groups; the latter normalizations permitted comparisons of the present values with the earlier reports cited in the Introduction. The absolute ventricular weights were similar between experimental groups or showed a slight fall in the diabetic animals. However, the values demonstrated relative myocardial hypertrophy when they were normalized to body weight. This was more pronounced in the animals in which diabetes was induced at an earlier age. Thus, *P* values derived from pair-wise significance testing against the controls (Table 2) indicated increases in normalized left and right ventricular weights. These increases were not significant in the animals made diabetic at 13 weeks (increases of 2.1 and 3.3 % for the left and right ventricles, respectively, relative to the controls) but were significant in animals made diabetic at 7 (24.9 and 25 %, respectively) and 10 weeks (15.3 and 10 %, respectively). In contrast, Table 4 demonstrates that captopril treatment abolished these changes: normalized left and right ventricular weights were then indistinguishable from the control values and accordingly significantly improved over values in the corresponding diabetic rats not treated with captopril.

Table 4. Basic physiological and MRI-myocardial volumes of the captopril-treated group diabetic from 7 weeks

Parameter	Value	*P*
Body weight at disease induction (g)	260 ± 10.6 †	NA
Body weight at scanning time (g)	247.5 ± 15.5 *	< 0.001
Blood glucose (mM)	29.4 ± 1.2 *	< 0.001
Systolic blood pressure (mmHg)	137.5 ± 7.5 ‡	0.006
Heart rate (beats min^{-1})	311 ± 10	0.017
Left ventricular weight (g)	0.463 ± 0.02 *‡	< 0.001
Right ventricular weight (g)	0.148 ± 0.008 *‡	< 0.001
LVMV (μl)	448.8 ± 20.1 *‡	< 0.001
RVMV (μl)	147 ± 11.9 *	0.004
Left ventricular weight/body weight (%)	0.188 ± 0.009 ‡	< 0.001
Right ventricular weight/body weight (%)	0.06 ± 0.0005 ‡	< 0.001
LVMV/ body weight (μl g^{-1})	1.82 ± 0.05 ‡	< 0.001
RVMV/ body weight (μl g^{-1})	0.59 ± 0.01 ‡	< 0.001

LVMV, left ventricular myocardial volume; RVMV, right ventricular myocardial volume. NA, not applicable. All values are expressed as means ± S.E.M. One-way ANOVA was used to compare the control and the two groups made diabetic from 7 weeks (one group not treated with captopril and the other treated with captopril; $n = 4$ animals in each group) followed by Tukey's honestly significant difference test for pair-wise multiple comparisons. The body weight-normalized values were calculated using the corresponding body weight of the anaesthetized rat. A value of $P < 0.05$ was considered significant. * Significantly different from the control group. ‡ Significantly different from the similarly diabetic group spared captopril treatment. † Within accepted range of standard Wistar rat growth curves.

Transverse MRI cardiac sections

Figure 2 displays typical end-diastolic and -systolic cardiac sections through the widest regions of intact beating hearts in control rats (*A*), in rats not treated with captopril made diabetic from 13, 10, and 7 weeks (*B–D*, respectively), and in captopril-treated diabetic rats (*E*). These were acquired using a repeatable and consistent image slice positioning protocol: this ensured that 12 imaged transverse cardiac slices were acquired through a plane perpendicular to the principal cardiac axis that joins the cardiac apex to the aortic valve in each experimental rat. The prone animal was first positioned in the radiofrequency probe horizontally in the bore of the imaging gradient set with its craniocaudal axis along the main magnetic field axis of the superconducting magnet. A set typically of nine sagittal images of its thoracic cavity was acquired using an enlarged field of view (typically 7 cm × 7 cm). The sagittal image with the clearest cardiac representation was then used as a pilot image to derive preliminary transverse–coronal (TCX) multislice images. In turn, the transverse–coronal image offering the clearest cardiac representation was used as a pilot image to define a set of 12 imaging planes (transverse cardiac slices or sections) perpendicular to the principal cardiac axis which provided images of the left and right ventricles in their entirety. The epi- and endocardial borders of both ventricles in these selected slices at all 12 time points were then used for accurate and consistent quantitative analysis for comparisons between animals in different experimental groups.

The cine imaging protocol provided high-resolution anatomical images that clearly demarcated the boundaries between blood and the endocardial borders of both ventricles; this was useful for reliable morphometric measurements. The left ventricles resembled that of human hearts in the consistent circular symmetry of their epi- and endocardial borders in transverse section throughout the cardiac cycle and in all experimental groups. Accordingly, the quantitative measurements of left and right ventricular myocardial volumes treated the interventricular septum as part of the left ventricle (Crowley *et al.* 1997; Wise *et al.* 1998). In contrast, the right ventricle was defined as the crescent-shaped cardiac chamber with its myocardial wall meeting the left ventricular myocardial wall close to the diameter of the left ventricle.

The images that were acquired 8 ms after the trigger pulse from the electrocardiographic R wave demonstrated fully dilated end-diastolic ventricles. End-systole corresponding to the minimum cross-section in both ventricular cavities was reached synchronously at ~99 ms after the trigger pulse in controls, rats diabetic from 13 weeks and captopril-treated rats. In contrast, ventricles of rats diabetic from 7 and 10 weeks reached end-systole ~112 ms after the trigger pulse.

Ventricular myocardial volumes measured by MRI

The borders of both ventricles in each transverse image slice were interactively defined using the blood–myocardial

wall contrast to define the endocardial borders and the myocardial wall–thoracic cavity contrast for drawing the epicardial borders. The pixel numbers enclosed within each border were then converted into units of square millimetres. These borders were independently drawn 4 times for each image slice. Left and right ventricular epi- and endocardial volumes were then calculated for all 12 time points through the cardiac cycle from each of the selected 12 transverse cardiac sections. The mean of the four calculated volumes then represented the empirical volume. The myocardial volume of each ventricle was then derived for each of the 12 examined time points by subtracting the endocardial volume from the corresponding epicardial volume.

Tables 3 and 4 demonstrate that both absolute and normalized myocardial volumes deduced from MRI concurred with the post-mortem determinations (Tables 2 and 4). Tables 3 and 4 also summarize the results of pair-wise statistical testing of myocardial volumes obtained in different diabetic groups against the untreated controls. The absolute left ventricular myocardial volumes measured by MRI were reduced by 17.6, 7.8 and 2.4 % in animals diabetic from 7, 10 and 13 weeks, respectively, relative to the control group and by 31.1 % with captopril treatment. The changes were significant in the two groups in which diabetes had been induced from 7 weeks with and without captopril treatment. The corresponding reductions in the absolute right ventricular myocardial volumes were 17.6,

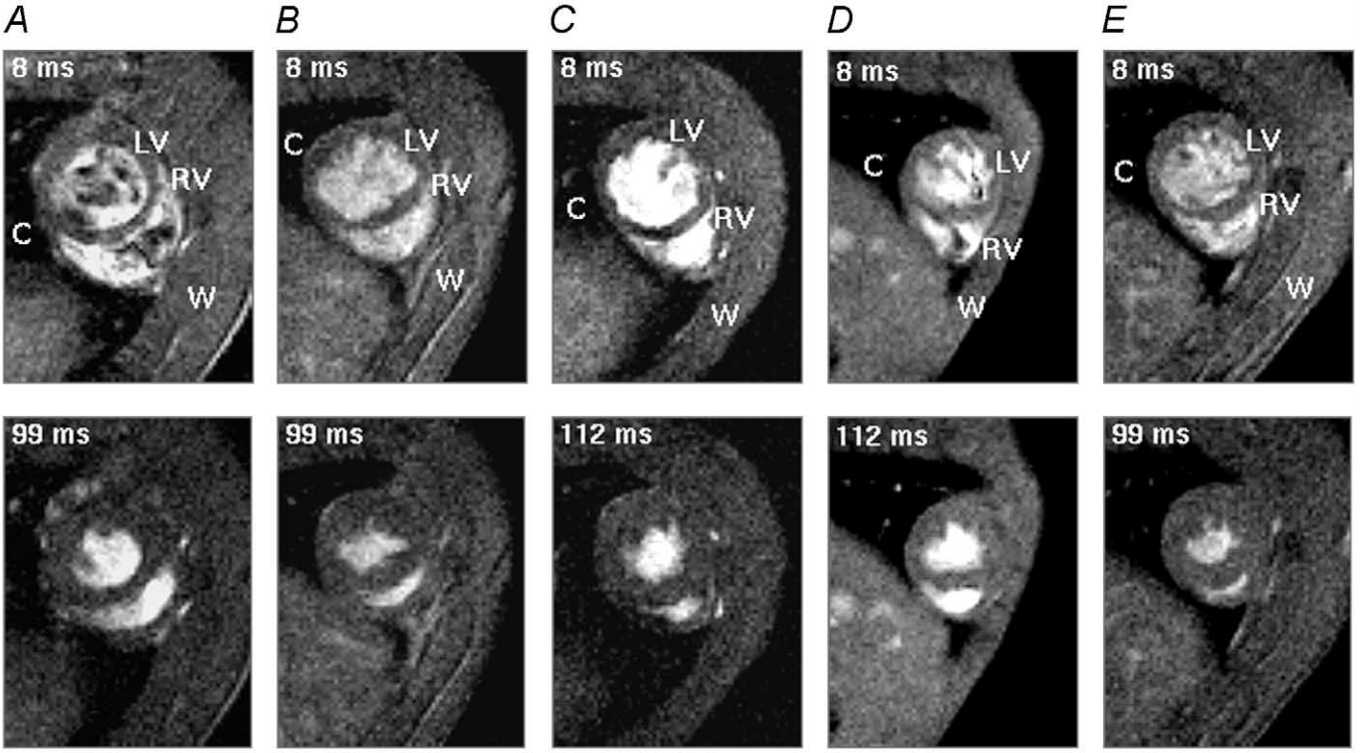

Figure 2. Transverse MRI sections

Typical transverse sections obtained in end-diastole (upper panel) and end-systole (lower panel) from the heart of a normal control rat (*A*), rats diabetic from 13 weeks (disease duration 3 weeks, *B*), 10 weeks (disease duration 6 weeks, *C*), 7 weeks (disease duration 9 weeks, *D*) and a captopril-treated rat diabetic from 7 weeks (disease duration 9 weeks, *E*). All rats were scanned when they were 16 weeks old. The body weight of the normal rat was 340 g and body weights of the rats diabetic from 7, 10 and 13 weeks and the captopril-treated rat were 230, 275, 330 and 245 g, respectively. The heart rate was continuously monitored throughout the imaging session giving an intrinsic heart rate of 315 ± 4 beats min^{-1} for the control rat and 290 ± 4, 300 ± 6, 307 ± 4 and 300 ± 4 beats min^{-1} for the four diabetic rats, respectively. The time points at which these images were taken are indicated in the upper left-hand corner of each panel and correspond to the delay after the trigger, taken from the R wave of the electrocardiogram (ECG), at which the signal was acquired. Each image is the average of two signals obtained at corresponding points in the cardiac cycle following the R wave. LV and RV indicate left and right ventricles, respectively, and C and W indicate chest cavity and chest wall, respectively. Slice thickness was 1.50 mm for the normal control rat and 1.44 mm for the four diabetic rats. Field of view (FOV) was 5 cm for the normal control rat and 4.5 cm for the four diabetic rats. With an image matrix of 128 × 128 pixels, the nominal in-plane resolution was approximately 351.6–390.6 μm $pixel^{-1}$. The effective repeat time (TR) was approximately 13 ms and the echo time (TE) was 4.3 ms.

11.6 and 3.0 %, respectively, and 28.3 % in the captopril-treated group.

However, the normalized left ventricular myocardial volumes showed increases of 23.1, 14.5 and 2.2 % in rats diabetic from 7, 10 and 13 weeks, respectively, relative to controls. The corresponding right ventricular values were 24.1, 10.3 and 1.7 %, respectively; in both cases, values from animals diabetic from 7 and 10 weeks were significantly elevated relative to controls. Captopril treatment prevented such changes. It left an actual 2.2 % decrease in normalized left ventricular myocardial volume and an insignificant 1.7 % increase in normalized right ventricular myocardial volume.

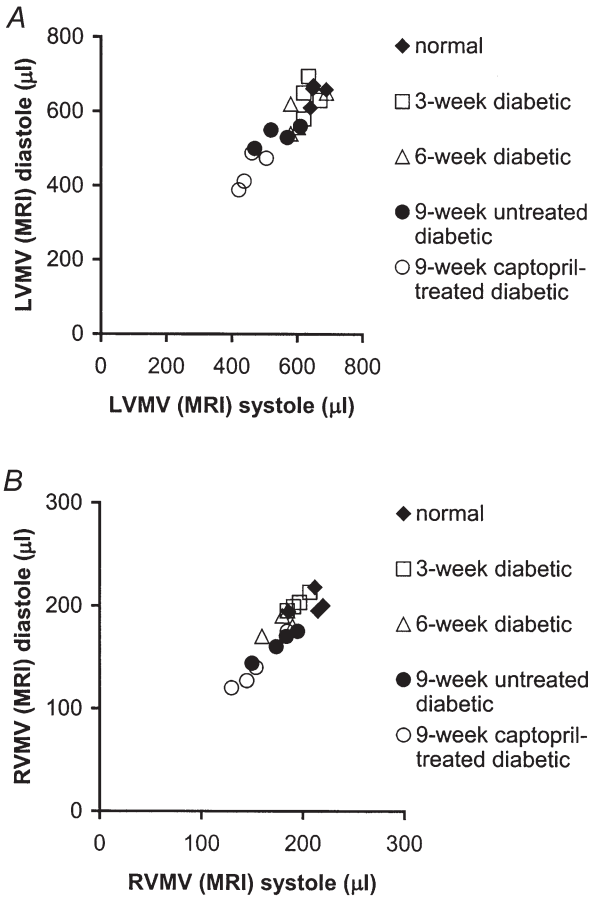

Figure 3. Conservation of left and right ventricular myocardial volumes through the cardiac cycle

A, the MRI-determined diastolic left ventricular (LV) myocardial volume (MV) plotted against its systolic value over 12 time points during the cardiac cycle for each rat. The left ventricular myocardial volume measured by MRI during systole, for each individual rat, was taken from the average value from all the time points sampled during systole. Similarly the left ventricular myocardial volume measured by MRI during diastole, for each individual rat, was taken from the average value from all the time points sampled during diastole in the cardiac cycle. Systolic and diastolic left ventricular myocardial volumes were closely correlated ($r = 0.91$). *B*, MRI-determined diastolic right ventricular (RV) myocardial volume plotted against its systolic value. Systolic and diastolic right ventricular myocardial volumes were also closely correlated ($r = 0.90$).

Internal consistency of MRI measurements

The images were made in rapidly beating hearts in which motion artefacts were minimized by gating the image acquisition to alternate electrocardiographic R waves. Nevertheless, a number of controls verified the MRI measurements made above and so the cine MRI methods introduced here provide a validated non-invasive quantitative analysis of cardiac changes in the rat MRI system that may permit serial studies in future. Firstly, the MRI-based measurements proved entirely internally self-consistent. Figure 3 plots the left and right ventricular myocardial volumes derived from the transverse sections during diastole against the corresponding volumes obtained during systole; a line of equality can be fitted through the data points.

Secondly, Fig. 4 demonstrates that the left and right ventricular myocardial volumes (μl) as determined by MRI were comparable with the left and right ventricular masses (in mg) in all five experimental groups measured directly at post mortem. The left and right ventricular myocardial densities calculated from these were closely comparable across all experimental groups. They gave an average ventricular myocardial density of 1.02 ± 0.02 mg μl^{-1} and 1.03 ± 0.02 mg μl^{-1} for the left and right ventricles, respectively, in agreement with previous reports (Wise *et al.* 1998).

DISCUSSION

The present experiments successfully introduced a cine-variant of MRI to detect, quantify and follow up chronic myocardial changes in both the left and right ventricles in experimental STZ-diabetic rats for the first time. There is a developing interest in the pathophysiology of diabetic cardiomyopathy and its associated haemodynamic abnormalities. The experiments introduced the non-invasive cardiac MRI techniques that have become accepted in clinical studies of cardiac disease but have yet to find wide applications in chronic physiological studies. In particular, they exploited ECG-gated cine-MRI of the heart; cine-MRI offers excellent contrast between the blood inside the cardiac chambers and the myocardium thereby providing clear demarcation of the cardiac cavities for quantitative analysis (Rehr *et al.* 1985; Higgins, 1986; Stratemeier *et al.* 1986; Caputo *et al.* 1987; Markiewicz *et al.* 1987; Pettigrew, 1989; Sechtem *et al.* 1987; Utz *et al.* 1987, 1988; Pflugfelder *et al.* 1989; Semelka *et al.* 1990). Experimental animal systems such as the widely used STZ-diabetic rat model, offer particular advantages as models for human disease as they permit chronic physiological changes to develop over a manageable and defined time scale, particularly when non-invasive imaging techniques

can both supplement or replace standard invasive physiological measurements.

The resolution and sensitivity of the MRI techniques permitted detection of early changes even in relatively small numbers of experimental rats and for them to be tracked over time, despite the high intrinsic heart rates. The latter required rapid image acquisition at closely incremented times through the cardiac cycle. MRI has already proven useful for similar high-resolution measurements of the major anatomical and functional clinical parameters of human cardiac performance (Stratemeier *et al.* 1986; Markiewicz *et al.* 1987; Sechtem *et al.* 1987; Semelka *et al.* 1990). Its successful use in the present physiological studies of the diabetic heart might thus lead to parallel human and animal MRI studies of ventricular function in this condition. This would aid physiological analysis of the increased morbidity and mortality that has been associated with human diabetic cardiomyopathy. Conversely, the non-invasive MRI procedures developed in rats would have potential application for the development of cardiac MRI in monitoring and detecting and studying human diabetic cardiac disease.

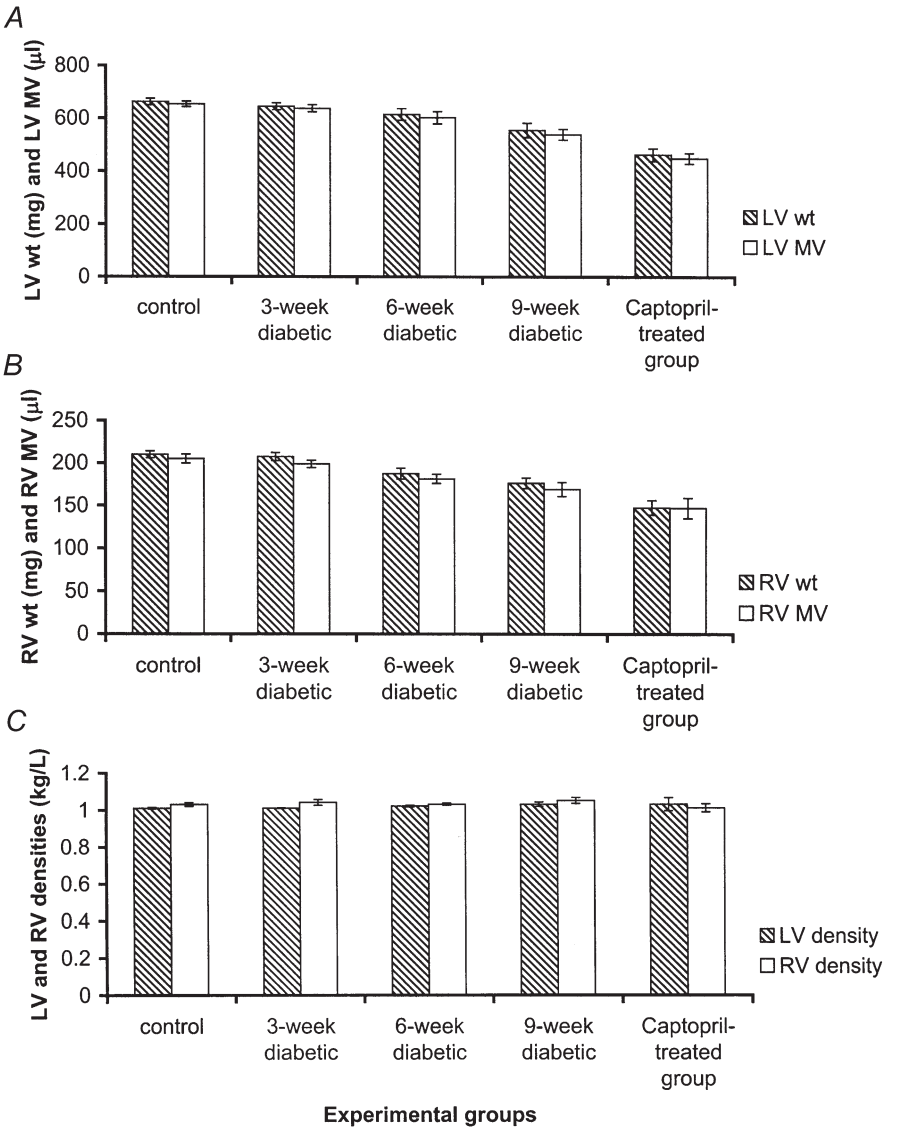

Figure 4. Consistency of measured left and right ventricular myocardial volumes

Plots of the MRI-determined left (*A*) and right (*B*) ventricular myocardial volumes (μl) against the corresponding directly determined left and right ventricular masses (mg) of the experimental groups measured post mortem. These give left ventricular myocardial densities (*C*) of 1.01 ± 0.004, 1.01 ± 0.002, 1.02 ± 0.005, 1.03 ± 0.01 and 1.03 ± 0.03 mg μl^{-1} and similar right ventricular myocardial densities of 1.03 ± 0.01, 1.04 ± 0.02, 1.03 ± 0.01, 1.05 ± 0.02 and 1.01 ± 0.02 mg μl^{-1} for control rats and the rats made diabetic at 13 (disease duration: 3 weeks), 10 (disease duration 6 weeks), 7 (disease duration 9 weeks) weeks, respectively, and captopril-treated (disease duration 9 weeks) diabetic rats, respectively.

The resulting data sets permitted complete anatomical reconstruction of the intact beating rat heart from data sets consisting of sets of 12 transverse sections obtained at 12 equally incremented times during the cardiac cycle. The experimental design used in association with the MRI studies examined groups of rats whose diabetes was induced at graded ages of 7, 10 and 13 weeks. All animals were then scanned at a consistent age of 16 weeks against a single age-matched control. Such timings meant that the present findings are comparable with earlier studies of the same experimental model that used independent, conventional invasive techniques. Earlier anatomical studies had examined for interstitial fibrosis (Factor *et al.* 1981) and ultrastructural myocardial changes (Jackson *et al.* 1985; Warley *et al.* 1995). Physiological studies had investigated papillary muscle function (Fein *et al.* 1980; Fein & Sonnenblick, 1994; Warley *et al.* 1995), myocardial contraction and relaxation (Jackson *et al.* 1985; Afzal *et al.* 1988), diastolic and peak systolic pressures (Afzal *et al.* 1988; Shimabukuro *et al.* 1995; Miller, 1979; Rodrigues & McNeill, 1986; Paulson *et al.* 1987; Rodrigues *et al.* 1988; Lopaschuk & Spafford, 1989; Goyal *et al.* 1998) and heart rates (Jackson & Carrier, 1983; Afzal *et al.* 1988; Maeda *et al.* 1995; Hicks *et al.* 1998) over similar age periods.

It proved possible reliably to extract from the images left and right ventricular myocardial volumes expressed both as absolute values and normalized to the corresponding body weights; the latter provided values in agreement with earlier studies on the STZ-diabetic model using conventional invasive anatomical methods (see Introduction for references). Firstly, the calculations of myocardial volumes were internally consistent: values of left and right ventricular myocardial volumes were closely similar at end-systole and -diastole in all five experimental groups. This expected conservation of both left and right ventricular myocardial volumes confirms that the determinations of the myocardial borders in each transverse MRI section and their reconstruction into myocardial volumes were consistent through the cardiac cycle. Secondly, at least some of the features deduced here agreed with available information from the conventional physiological and pathological studies cited above. Finally, the MRI measurements also closely correlated with the myocardial masses measured post mortem to give consistent values of myocardial densities that closely agreed with earlier studies, at least in normal rats: in the present study rats were killed immediately after imaging for histological analysis (Wise *et al.* 1998). The latter findings will make it possible to perform serial studies on such experimental systems in future without a requirement for such post-mortem corroboration.

The myocardial volume determinations demonstrated that the left and right ventricles both significantly hypertrophied relative to the corresponding body weights resulting in significant differences from control results in rats made diabetic from 7 and 10 weeks. This agrees with earlier pathological reports of myocardial hypertrophy and interstitial fibrosis in diabetic hearts and places such findings on a quantitative basis for the first time (Rubler *et al.* 1972; Fischer *et al.* 1979). They also corroborate clinical echocardiographic findings in humans of an increased left ventricular posterior wall and interventricular septal thicknesses in diabetics (Airaksinen *et al.* 1984, 1987). The present findings, to our knowledge, also constitute the first reports, whether human or animal, of *right* ventricular changes in diabetes; there are no corresponding echocardiographic reports concerning the right ventricle in diabetes. However, the present experiments demonstrated that ventricular changes took place at considerably earlier times than it would have been possible to demonstrate in clinical studies.

The present approach was finally used to evaluate the effects of the angiotensin-converting enzyme inhibitor captopril in preventing the myocardial abnormalities demonstrated here. It has been suggested that diabetes activates an intracardiac renin–angiotensin system (Dostal *et al.* 1992*a*,*b*; Rösen *et al.* 1995; Goyal *et al.* 1998) from which elevated angiotensin II production might induce the growth responses and hypertrophy (Schunkert *et al.* 1995; LaMorte *et al.* 1994) as well as the cardiac fibroblast proliferation and consequent myocardial interstitial fibrosis (Schorb *et al.* 1993, 1994; Crabos *et al.* 1994; Matsubara *et al.* 1994) reported in some forms of cardiac hypertrophy and cardiomyopathy. The experiments provided the first non-invasive physiological evidence that the ACE inhibitor captopril ameliorates the myocardial hypertrophic changes. Thus, the captopril-treated diabetic rats showed no such ventricular hypertrophy, suggesting a therapeutic effect of captopril on the development of experimental diabetic cardiomyopathy. Earlier reports described therapeutic benefits of ACE inhibitors in relieving left ventricular and other vascular abnormalities in other forms of systemic cardiovascular disease (Cohn & Levine, 1982; Kluger *et al.* 1982; Levine *et al.* 1982; Dunn *et al.* 1984; Dzau & Safar, 1988; Mulvany, 1992, 1998). The present findings justify testing for similar therapeutic physiological effects in diabetic cardiac disease, in addition to providing the MRI techniques necessary for the more detailed analyses of cardiac cycle changes in the STZ-diabetes cardiac model detailed in the accompanying paper (Al-Shafei *et al.* 2002).

REFERENCES

Afzal, N., Ganguly, P. K., Dhalla, K. S., Pierce, G. N., Signal, P.K. & Dhalla, N. S. (1988). Beneficial effects of verapamil in diabetic cardiomyopathy. *Diabetes* **37**, 937–942.

Airaksinen, K. E. J., Ikäheimo, M., Kaila, J., Linnaluoto, M. & Takkumen, J. (1984). Impaired left ventricular filling in young female diabetics. An echocardiographic study. *Acta Medica Scandinavica* **216**, 509–516.

Airaksinen, K. E. J., Ikäheimo, M. J., Linnaluoto, M. K., Huikuri, H. V. & Takkumen, J. T. (1987). Increased left atrial size relative to left ventricular size in young women with insulin dependent diabetes: a pre-clinical sign of the specific heart disease of diabetes? *Diabetes Research* **6**, 37–41.

Al-Shafei, A. I. M., Wise, R. G., Gresham, G. A., Carpenter, T. A., Hall, L. D. & Huang, C. L.-H. (2002). Magnetic resonance imaging analysis of cardiac cycle events in diabetic rats: the effect of angiotensin-converting enzyme inhibition. *Journal of Physiology* **538**, 555–572.

Ballon, D., Graham, M. C., Midownik, S. & Koutcher, J. A. (1990). A 64 MHz half-birdcage resonator for clinical imaging. *Journal of Magnetic Resonance* **90**, 131–140.

Bell, D. S. (1995). Diabetic cardiomyopathy. A unique entity or a complication of coronary artery disease? *Diabetes Care* **18**, 708–714.

Blumenthal, H. T., Alex, M. & Goldenberg, S. (1960). A study of lesions of intramural coronary artery branches in diabetes mellitus. *Archives of Pathology* **70**, 13–28.

Caputo, G. R., Tscholakoff, D., Sechtem, U. & Higgins, C. B. (1987). Measurement of canine left ventricular mass by using MR imaging. *American Journal of Roentgenology* **148**, 33–38.

Cohn, J. N. & Levine, T. B. (1982). Angiotensin-converting enzyme inhibition in congestive heart failure: the concept. *American Journal of Cardiology* **49**, 1480–1483.

Crabos, M., Roth, M., Hahn, A. W. & Erne, P. (1994). Characterization of angiotensin II receptors in cultured adult rat cardiac fibroblasts. Coupling to signalling systems and gene expression. *Journal of Clinical Investigation* **93**, 2372–2378.

Crall, F. V. Jr & Roberts, W. C. (1978). The extramural and intramural coronary arteries in juvenile diabetes mellitus. Analysis of nine necropsy patients aged 19 to 38 years with onset of diabetes before age 15 years. *American Journal of Medicine* **64**, 221–230.

Crowley, J. J., Huang, C. L., Gates, A. R., Basu, A., Shapiro, L. M., Carpenter, T. A. & Hall, L. D. (1997). A quantitative description of dynamic left ventricular geometry in anaesthetized rats using magnetic resonance imaging. *Experimental Physiology* **82**, 887–904.

Dalton, G. R., Jones, J. V., Evans, S. J. & Levi, A. J. (1997). Wall stress-induced arrhythmias in the working rat heart as left ventricular hypertrophy regresses during captopril treatment. *Cardiovascular Research* **33**, 561–572.

Dostal, D. E., Rothblum, K. N., Chernin, M. I., Cooper, G. R. & Baker, K. M. (1992*a*). Intracardiac detection of angiotensinogen and renin: a localized renin-angiotensin system in neonatal rat heart. *American Journal of Physiology* **263**, C838–850.

Dostal, D. E., Rothblum, K. N., Conrad, K. M., Cooper, G. R. & Baker, K. M. (1992*b*). Detection of angiotensin I and II in cultured rat cardiac myocytes and fibroblasts. *American Journal of Physiology* **263**, C851–863.

Dunn, F. G., Oigman, W., Ventura, H. O., Messerli, F. H., Kobrin, I. & Frohlich, E. D. (1984). Enalapril improves systemic and renal hemodynamics and allows regression of left ventricular mass in essential hypertension. *American Journal of Cardiology* **53**, 105–108.

Dzau, V. J. & Safar, M. E. (1988). Large conduit arteries in hypertension: role of the vascular renin-angiotensin system. *Circulation* **77**, 947–954.

Factor, S. M., Bhan, R., Minase, T., Wolinsky, H. & Sonnenblick, E. H. (1981). Hypertensive-diabetic cardiomyopathy in the rat: an experimental model of human disease. *American Journal of Pathology* **102**, 219–228.

Fein, F. S., Kornstein, L. B., Strobeck, J. E., Capasso, J. M. & Sonnenblick, E. H. (1980). Altered myocardial mechanics in diabetes. *Circulation Research* **47**, 922–933.

Fein, F. S. & Sonnenblick, E. H. (1994). Diabetic cardiomyopathy. *Cardiovascular Drugs and Therapy* **8**, 65–73.

Feuvray, D., Idell Wenger, J. A. & Neely, J. R. (1979). Effects of ischemia on rat myocardial function and metabolism in diabetics. *Circulation Research* **44**, 322–329.

Fischer, V. W., Barner, H. B. & Leskiw, M. L. (1979). Capillary basal laminar thickness in diabetic human myocardium. *Diabetes* **28**, 713–719.

Friedman, N. E., Levitsky, L. L., Edidin, D. V., Vitullo, D. A., Lacina, S. J. & Chiemmongkolti, P. (1982). Echocardiographic evidence for impaired myocardial performance in children with type 1 diabetes mellitus. *American Journal of Medicine* **73**, 846–850.

Garcia, M. J., Mcnamara, P. M., Gordon, T. & Kannel, W. B. (1974). Morbidity and mortality in diabetics in the Framingham population. Sixteen year follow-up study. *Diabetes* **23**, 105–111.

Goodwin, J. F. & Oakley, C. M. (1972). The cardiomyopathies. *British Heart Journal* **34**, 545–552.

Goyal, R. K., Satia, M. C., Bangaru, R. A. & Gandhi, T. P. (1998). Effect of long-term treatment with enalapril in streptozotocin diabetic and DOCA hypertensive rats. *Journal of Cardiovascular Pharmacology* **32**, 317–322.

Hamby, R. I., Zoneraich, S. & Sherman, S. (1974). Diabetic cardiomyopathy. *Journal of the American Medical Association.* **229**, 1749–1754.

Hearse, D. J., Stewart, D. A. & Chain, E. B. (1975). Diabetes and the survival and recovery of the anoxic myocardium. *Journal of Molecular and Cellular Cardiology* **7**, 397–415.

Hicks, K. K., Seifen, E., Stimers, J. R. & Kennedy, R. H. (1998). Effects of streptozotocin-induced diabetes on heart rate, blood pressure and cardiac autonomic nervous control. *Journal of the Autonomic Nervous System* **69**, 21–30.

Higgins, C. B. (1986). Overview of MR of the heart. *American Journal of Roentgenology* **146**, 907–918.

Jackson, C. V. & Carrier, G. O. (1983). Influence of short-term experimental diabetes on blood pressure and heart rate in response to norepinephrine and angiotensin II in the conscious rat. *Journal of Cardiovascular Pharmacology* **5**, 260–265.

Jackson, C. V. McGrath, G. M., Tahiliani, A. G., Vadalmudi, R. V. S. V. & McNeill, J. H. (1985). A functional and ultrastructural analysis of experimental diabetic rat myocardium: Manifestation of a cardiomyopathy. *Diabetes* **34**, 876–883.

Junod, A., Lambert, A. E., Orci, L., Pictet, R., Gonet, A. E. & Renold, A. E. (1967). Studies of the diabetogenic action of streptozotocin. *Proceedings of the Society for Experimental Biology and Medicine* **126**, 201–205.

Junod, A., Lambert, A. E., Stauffacher, W. & Renold, A. E. (1969). Diabetogenic action of streptozotocin: relationship of dose to metabolic response. *Journal of Clinical Investigation* **48**, 2129–2139.

Kannel, W. B. (1985). Lipids, diabetes, and coronary heart disease: insights from the Framingham Study. *American Heart Journal* **110**, 1100–1107.

Kannel, W. B., Hjotland, M. & Castelli, W. P. (1974). Role of diabetes in congestive heart failure: the Framingham study. *American Journal of Cardiology* **34**, 29–34.

Kannel, W. B. & McGee, D. L. (1979). Diabetes and cardiovascular disease. The Framingham study. *Journal of the American Medical Association* **241**, 2035–2038.

Kluger, J., Cody, R. J. & Laragh, J. H. (1982). The contributions of sympathetic tone and the renin-angiotensin system to severe chronic congestive heart failure: response to specific inhibitors (prazosin and captopril). *American Journal of Cardiology* **49**, 1667–1674.

LaMorte, V. J., Thorburn, J., Absher, D., Spiegel, A., Brown, J. H., Chien, K. R., Feramisco, J. R. & Knowlton, K.U. (1994). Gq- and ras-dependent pathways mediate hypertrophy of neonatal rat ventricular myocytes following alpha 1-adrenergic stimulation. *Journal of Biological Chemistry* **269**, 13490–13496.

Ledet, T. (1968). Histological and histochemical changes in the coronary arteries of old diabetic patients. *Diabetologia* **4**, 268–272.

Ledet, T. (1976). Diabetic cardiopathy. Quantitative histological studies of the heart from young juvenile diabetics. *Acta Pathologica et Microbiologica Scandinavica* (*A*) **84**, 421–428.

Ledet, T., Neubauer, B., Christenson, N. J. & Lundback, K. (1979). Diabetic cardiopathy. *Diabetologia* **16**, 207–209.

Levine, T. B., Francis, G. S., Goldsmith, S. R., Simon, A. B. & Cohn, J. N. (1982). Activity of the sympathetic nervous system and renin-angiotensin system assessed by plasma hormone levels and their relation to hemodynamic abnormalities in congestive heart failure. *American Journal of Cardiology* **49**, 1659–1666.

Lopaschuk, G. D. & Spafford, M. (1989). Response of isolated working hearts to fatty acids and carnitine palmitoyltransferase I inhibition during reduction of coronary flow in acutely and chronically diabetic rats. *Circulation Research* **65**, 378–387.

Lopaschuk, G. D., Tahiliani, A. G., Vadlamudi, R. V., Katz, S. & McNeill, J. H. (1983). Cardiac sarcoplasmic reticulum function in insulin- or carnitine-treated diabetic rats. *American Journal of Physiology* **245**, H969–976.

Maeda, C. Y., Fernandes, T. G., Lulhier, F. & Irigoyen, M. C. (1995). Streptozotocin diabetes modifies arterial pressure and baroreflex sensitivity in rats. *Brazilian Journal of Medical and Biological research* **28**, 497–501.

Malhotra, A., Penpargkul, S., Fein, F. S., Sonnenblick, E. H. & Scheuer, J. (1981). The effect of streptozotocin-induced diabetes in rats on cardiac contractile proteins. *Circulation Research* **49**, 1243–1250.

Markiewicz, W., Sechtem, U. & Higgins, C. B. (1987). Evaluation of the right ventricle by magnetic resonance imaging. *American Heart Journal* **113**, 8–15.

Matsubara, H., Kanasaki, M., Murasawa, S., Tsukaguchi, Y., Nio, Y. & Inada, M. (1994). Differential gene expression and regulation of angiotensin II receptor subtypes in rat cardiac fibroblasts and cardiomyocytes in culture. *Journal of Clinical Investigation* **93**, 1592–1601.

Miller, T. B. Jr (1979). Cardiac performance in isolated perfused hearts from alloxan diabetic rats. *American Journal of Physiology* **230**, H808–812.

Mulvany, M. J. (1992). Effects of angiotensin converting enzyme inhibition on vascular remodelling of resistance vessels in hypertensive patients. *Journal of Hypertension* **14** (suppl. 6), 21–24.

Mulvany, M. J. (1998). Effects of angiotensin-converting enzyme inhibition on vascular remodeling of resistance vessels in hypertensive patients. *Metabolism* **47** (suppl. 1), 20–23.

Paulson, D. J., Kopp, S. J., Peace, D. G. & Tow, J. P. (1987). Myocardial adaptation to endurance exercise training in diabetic rats. *American Journal of Physiology* **252**, R1073–1081.

Paz-Guevara, A. T., Hsu, T. H. & White, P. (1975). Juvenile diabetes mellitus after forty years. *Diabetes* **24**, 559–565.

Pettigrew, R. I. (1989). Dynamic cardiac MR imaging. Techniques and applications. *Radiologic Clinics of North America* **27**, 1183–1203.

Pflugfelder, P. W., Landzberg, J. S., Cassidy, M. M., Cheitlin, M. D., Schiller, N. B., Auffermann, W. & Higgins, C. B. (1989). Comparison of cine MR imaging with Doppler echocardiography for the evaluation of aortic regurgitation. *American Journal of Roentgenology* **152**, 729–735.

Pierce, G. N. & Dhalla, N. S. (1981). Cardiac myofibrillar ATPase activity in diabetic rats. *Journal of Molecular and Cellular Cardiology* **13**, 1063–1069.

Pierce, G. N. & Dhalla, N. S. (1983). Sarcolemmal Na^+-K^+-ATPase activity in diabetic rat heart. *American Journal of Physiology* **245**, C241–247.

Pierce, G. N. & Dhalla, N. S. (1985*a*). Mechanisms of defect in cardiac myofibrillar function during diabetes. *American Journal of Physiology* **248**, E170–175.

Pierce, G. N. & Dhalla, N. S. (1985*b*). Mitochondrial abnormalities in diabetic cardiomyopathy. *Canadian Journal of Cardiology* **1**, 48–54.

Qi, X. L., Stewart, D. J., Gosselin, H., Azad, A., Picard, P., Andries, L., Sys, S. U., Brutsaert, D. L. & Rouleau, J. L. (1999). Improvement of endocardial and vascular endothelial function on myocardial performance by captopril treatment in postinfarct rat hearts. *Circulation* **100**, 1338–1345.

Regan, T. J., Ettinger, P. O., Khan, M. I., Jesrani, M. U., Lyons, M. M., Oldewurtel, H. A. & Weber, M. (1974). Altered myocardial function and metabolism in chronic diabetes mellitus without ischaemia in dogs. *Circulation Research* **35**, 222–237.

Regan, T. J., Wu, C. F., Yeh, C. K., Oldewurtel, H. A. & Haider, B. (1981). Myocardial composition and function in diabetes: the effect of chronic insulin use. *Circulation Research* **49**, 1268–1277.

Rehr, R. B., Malloy, C. R., Filipchuk, N. G. & Peshock, R. M. (1985). Left ventricular volumes measured by MR imaging. *Radiology* **156**, 717–719.

Riva, E., Andreoni, G., Bianchi, R., Latini, R., Luvarà, G., Jeremic, G., Traquandi, C. & Tuccinardi, L. (1998). Changes in diastolic function and collagen content in normotensive and hypertensive rats with long-term streptozotocin-induced diabetes. *Pharmacological Research* **37**, 233–240.

Rodrigues, B., Cam, M. C., Kong, J., Goyal, R. K. & Mcneill, J. H. (1997). Strain differences in susceptibility to streptozotocin-induced diabetes: Effects on hypertriglyceridemia and cardiomyopathy. *Cardiovascular Research* **34**, 199–205.

Rodrigues, B. & McNeill, J. H. (1986). Cardiac function in spontaneously hypertensive diabetic rats. *American Journal of Physiology* **251**, H571–580.

Rodrigues, B., Ross, J. R., Farahbakshian, S. & McNeill, J. H. (1990). Effects of in vivo and in vitro treatment with L-carnitine on isolated hearts from chronically diabetic rats. *Canadian Journal of Physiology and Pharmacology* **68**, 1085–1092.

Rodrigues, B., Xiang, H. & McNeill, J. H. (1988). Effect of L-carnitine treatment on lipid metabolism and cardiac performance in chronically diabetic rats. *Diabetes* **37**, 1358–1364.

Rösen, R., Rump, A. F. & Rösen, P. (1995). The ACE-inhibitor captopril improves myocardial perfusion in spontaneously diabetic (BB) rats. *Diabetologia* **38**, 509–517.

Rubler, S., Dlugash, J., Yuceoglu, Y. Z., Kumral, T., Branwood, A. W. & Grisham, A. (1972). New type of cardiomyopathy associated with diabetic glomerulosclerosis. *American Journal of Cardiology* **30**, 595–602.

Sanderson, J. E., Brown, D. J., Rievellese, A. & Kohner, E. (1978). Diabetic cardiomyopathy? An echocardiographic study of young diabetics. *British Medical Journal* **1**, 404–407.

Schorb, W., Booz, G. W., Dostal, D. E., Conrad, K. M., Chang, K. C. & Baker, K. M. (1993). Angiotensin II is mitogenic in neonatal rat cardiac fibroblasts. *Circulation Research* **72**, 1245–1254.

Schorb, W., Peeler, T. C., Madigan, N. N., Conrad, K. M. & Baker, K. M. (1994). Angiotensin II-induced protein tyrosine phosphorylation in neonatal rat cardiac fibroblasts. *Journal of Biological Chemistry* **269**, 19626–19632.

Schunkert, H., Sadoshima, J., Cornelius, T., Kagaya, Y., Weinberg, E. O., Izumo, S., Riegger, G. & Lorell, B. H. (1995). Angiotensin II-induced growth responses in isolated adult rat hearts. Evidence for load-independent induction of cardiac protein synthesis by angiotensin II. *Circulation Research* **76**, 489–497.

Sechtem, U., Pflugfelder, P. W., Gould, R. G., Cassidy, M. M. & Higgins, C. B. (1987). Measurement of right and left ventricular volumes in healthy individuals with cine MR imaging. *Radiology* **163**, 697–702.

Semelka, R. C., Tomei, E., Wagner, S., Mayo, J., Kondo, C., Suzuki, J., Caputo, G. R. & Higgins, C. B. (1990). Normal left ventricular dimensions and function: interstudy reproducibility of measurements with cine MR imaging. *Radiology* **174**, 763–768.

Seneviratne, B. I. (1977). Diabetic cardiomyopathy: the preclinical phase. *British Medical Journal* **l**, 1444–1446.

Shapiro, L. M., Howat, A. P. & Calter, M. M. (1981). Left ventricular function in diabetes mellitus: II: Relation between clinical features and left ventricular function. *British Heart Journal* **45**, 129–132.

Shimabukuro, M., Shinzato, T., Higa, S., Nagamine, F., Murakami, K. & Takasu, N. (1995). Impaired mechanical response to calcium of diabetic rat hearts–Reversal by nifedipine treatment. *Journal of Cardiovascular Pharmacology* **26**, 495–502.

Stratemeier, E. J., Thompson, R., Brady, T. J., Miller, S. W., Saini, S., Wismer, G. L., Okada, R. D. & Dinsmore R. E. (1986). Ejection fraction determination by MR imaging: comparison with left ventricular angiography. *Radiology* **158**, 775–777.

Utz, J. A., Herfkens, R. J., Heinsimer, J. A., Bashore, T., Califf, R., Glover, G., Pelc, N. & Shimakawa, A. (1987). Cine MR determination of left ventricular ejection fraction. *American Journal of Roentgenology* **148**, 839–843.

Utz, J. A., Herfkens, R. J., Heinsimer, J. A., Shimakawa, A., Glover, G. & Pelc, N. (1988). Valvular regurgitation: dynamic MR imaging. *Radiology* **168**, 91–94.

Vracko, R. & Benditt, E. P. (1970). Capillary basal lamina thickening: its relationship to endothelial cell death and replacement. *Journal of Cell Biology* **47**, 281–285.

Warley, A., Powell, J. M. & Skepper, J. N. (1995). Capillary surface area is reduced and tissue thickness from capillaries to myocytes is increased in the left ventricle of streptozotocin-diabetic rats. *Diabetologia* **38**, 413–421.

Weber, K. T. & Brilla, C. G. (1991). Pathological hypertrophy and cardiac interstitium. Fibrosis and renin-angiotensin-aldosterone system. *Circulation* **83**, 1849–1865.

Williamson, J. R. & Kilo, C. (1976). Basement-membrane thickening and diabetic microangiopathy. *Diabetes* **25** (suppl. 2), 925–927.

Wise, R. G., Huang, C. L.-H., Gresham, G. A., Al-Shafei, A. I. M., Carpenter, T. A. & Hall, L. D. (1998). Magnetic resonance imaging analysis of left ventricular function in normal and spontaneously hypertensive rats. *Journal of Physiology* **513**, 873–887.

Zoneraich, S., Silverman, G. & Zonereich, O. (1980). Primary myocardial disease, diabetes mellitus, and small vessel disease. *American Heart Journal* **100**, 754–755.

Acknowledgements

The authors thank Dr Herchel Smith for his generous endowment, which supports the Herchel Smith Laboratory. A.I.M.A.-S. also thanks the Karim Rida Said Foundation for scholarship support. R.G.W. thanks the Wellcome Trust for his Research Training Studentship in Mathematical Biology. C.L-H.H., T.A.C. and L.D.H. acknowledge project grant funding from the BBSRC and Joint Research Equipment Initiative (JREI) support from the MRC. Special thanks are given to Mr Simon Smith for technical assistance. C.L-H.H. also thanks the Royal Society for funding support.